Int. J. Electrochem. Sci., 8 **(2013)** 1903 - 1910

International Journal of
ELECTROCHEMICAL
SCIENCE
www.electrochemsci.org

Short Communication

Electrodeposition Synthesis of Au-Cu Heterojunction Nanowires and Their Optical Properties

Xue Zhao, Yongzhong Wu[*], *Xiaopeng Hao*[*]

State Key Laboratory of Crystal Materials, Shandong University, Jinan 250100, P.R. China
[*]E-mail: xphao@sdu.edu.cn; wuyz@sdu.edu.cn

Received: 28 December 2012 / *Accepted:* 19 January 2013 / *Published:* 1 February 2013

Au-Cu heterojunction nanowires with different diameters were fabricated with assistance of the anodic alumina oxide (AAO) template by electrochemical deposition. The as-prepared nanowires were characterized by means of scanning electron microscopy (SEM), X-ray diffraction (XRD), energy dispersive X-ray spectrometer (EDS) and reflected laser confocal imaging. Optical properties of the Au-Cu heterojunction nanowires were studied. In UV-visible absorption spectra, Au-Cu heterojunction nanowires exhibit enhanced absorption compared with single Au and Cu nanowires, and the absorption bands are broadening and red shifted, which are attributed to the electron transfer between Au and Cu segments.

Keywords: Au-Cu heterojunction nanowires; electrodeposition; absorption spectra; electron transfer

1. INTRODUCTION

One-dimensional metallic nanostructures such as nanorods, nanowires and nanotubes have attracted considerable attention due to their unique structures and spectacular optical, electrical and magnetic properties [1-5]. Since one-dimensional nanostructures are being used in a wide range, a natural progression has been towards the synthesis and design of more complex, multicomponent materials to perform many functions simultaneously. Heterostructured metallic nanowires with multiple functionalities and unique properties not realized in their monometallic counterparts due to the coupling effect of different metal components have been extensively developed [4, 6-9]. Multi-segmented nanowires composed of thin Co-Cu [5, 10] and NiFe-Cu [10, 11] layers exhibit giant magnetoresistance due to the interaction between different metal layers. Heterojunction nanowires synthesized with catalytically active components such as Pt and Ni can have their maximum electrocatalytic effects [12-14]. The striped metallic nanorods can be employed as nanobarcodes which are applied to multiplexed detection and sensing of biological analytes [15-17].

Au-Cu heterojunction nanomaterials have been of great interest due to their wide range of applications. For example, Au-Cu heterojunction nanostructures with controlled shape and size are necessary for device integration and fundamental structure-property studies. Au-Cu bimetallic nanomaterials exhibit excellent catalytic activity, such as selective oxidation of benzyl alcohol, low-temperature CO oxidation and epoxidation of propene [18-20]. However, compared to mono-component nanowires, the synthesis of heterostructured metal nanowires with controllable composition and geometry remains a great challenge due to the different growth parameters. For instance, spherical Au-Cu nanoparticles with different compositions and Au-Cu alloy nanorods were successfully prepared by using a seed-based method [21, 22]. Liu et al. [23] have prepared uniform, single-crystalline Au-Cu nanocubes with the polyol reduction method. Schaak [24] and Zhang [25] synthesized Au-Cu nanowire networks separately with accurate control of high temperature or wet chemical route with assistance of capping agent. Compared with the listed methods above, electrodeposition can be used to deposit Au-Cu heterojunction nanowires conveniently into nanopores such as AAO templates without addition of crystal seed, reducing agent or capping agent and high temperature. Electrodeposition synthesis is simple and the process has a low cost and high efficiency. It enables excellent control over the geometry and chemical compositions by changing the plating solution and varying the potential of deposition. Electrochemical deposition does not require expensive instrumentation, high temperatures or low-vacuum pressures. Till now, electrodeposition combined with AAO template has been one of the most successful methods for the preparation of one-dimensional heterojunction nanostructures [26, 27].

Although some progresses have been made in the preparation of Au-Cu bimetallic nanosrtructures, there are few reports about the controlled synthesis of Au-Cu one-dimensional heterojunction nanowires. To the best of our knowledge, Kim and co-workers [28] fabricated the Au-Cu-Ni multi-segmented nanowires with assistance of electrodeposition, but no properties were further investigated. In this paper, orderly and uniform Au-Cu heterojunction nanowires were fabricated by AAO template with different diameters by electrodeposition technology. The as-prepared nanowires were characterized by means of SEM, XRD, EDS and reflected laser confocal imaging. UV-visible absorption spectra of the Au-Cu heterojunction nanowires were investigated. Au-Cu heterojunction nanowires exhibit enhanced and broadening absorption compared with single Au and Cu nanowires, which are attributed to the electron transfer between Au and Cu segments.

2. EXPERIMENTAL PROCEDURE

2.1. Synthesis procedure

The anodic aluminum oxide membranes (AAO) were purchased from Whatman, and the nominal diameter (d_N) are 100 nm and 20 nm specified by the manufacturer. A layer of gold film serving as back electrode was electron-beam evaporated onto one side of the AAO membrane. A thick layer of Au was needed in case of the wide pores to ensure that the electrode completely covered the pores [29]. After evaporation, the membrane was fixed with the Au electrode facing down onto a

conducting substrate (aluminum foil in our experiment) using an adhesive sticker. A bundle of Cu wires was applied to introduce the electrode to the deposition system. Nail polish was smeared on the aluminum foil and around the AAO to isolate electrolyte from undesired deposition. Electrodeposition was conducted in a Teflon cell by a three-electrode system. There was no separate compartment for the counter electrode which was a Pt plate, nor was there any stirring or heating. A saturated calomel electrode (SCE) was employed as reference electrode for the applied potential. Using a conventional potentiostat, the current was measured during electroplating at a fixed potential versus SCE, referred to as V_{SCE}.

All chemicals were commercially available and utilized as received without further purification unless otherwise stated. Au segments were grown from an electrolyte that contained 4 g L^{-1} $HAuCl_4 \cdot 4H_2O$ (99.99%, Alfa-Aesar) and 3.71 g L^{-1} H_3BO_3. Cu segments were deposited from 125 g L^{-1} $CuSO_4 \cdot 5H_2O$ and 30 g L^{-1} H_3BO_3. The pH values of both electrolytes were adjusted to 3-4 by HNO_3. Au segments and Cu segments were separately deposited at constant potentials of -1.0 V and -0.3 V. After electrodeposition, the AAO membrane was removed in 20 g L^{-1} NaOH solution and the prepared sample was washed with distilled water for three times before drying. Due to protecting of nail polish, the AAO was etched only from top-side of the nanowires, which could keep a good morphology of Au-Cu heterojunction nanowires.

2.2. Structural and morphological characterization

The heterojunction nanowires were characterized by using field-emission scanning electron microscopy (FESEM, HITACHI S4800, Japan), energy dispersive x-ray spectrometer (EDS, HORIBA EMAX Energy EX-450, Japan) and X-ray diffraction (XRD, Bruker/D8-advance with Cu Kα radiation (λ = 1.54178 Å), Germany). The UV-visible absorption spectra were measured using a Shimadzu UV-2550 spectrophotometer with an integrating sphere in ambient conditions. Reflected laser confocal image of an individual Au-Cu heterojunction nanowire was taken on NT-MDT NTEGRA Spectra of Russia using a 488nm laser.

3. RESULTS AND DISCUSSIONS

Au-Cu heterojunction nanowires were obtained by simple electrochemistry deposition within the AAO template of d_N = 100 nm. Morphology and element distribution patterns of the as-prepared Au-Cu nanowires are exhibited in Fig. 1. The nanowires are well-ordered, uniform and with a high density, whose diameter and length are about 260 nm and 12 μm, respectively. The synthesized nanowires have topological morphology at the bottom part which is determined by AAO template and it is similar to the morphology in Forrer's experiment [30]. The Au-Cu heterojunction nanowires show one sharp interface between the dark contrast Cu segments and the light Au segments, which shows similar situation to the CoPtP/Au multisegment nanowires [31]. Au and Cu segments are well connected and the lengths of which are separately about 2 μm and 10μm. The EDS patterns in Fig. 1b

and Fig. 1c are corresponding to the marks at the Cu segments and Au segments of the Au-Cu nanowires.

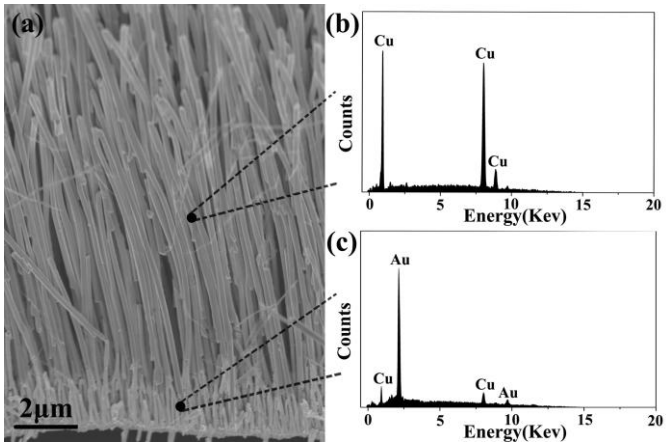

Figure 1. SEM image (a) and EDS patterns (b) (c) of the as-prepared Au-Cu heterojunction nanowires from d_N = 100 nm AAO

Characteristic X rays of Cu element are exhibited in Fig. 1b. It is observed that there are two weak peaks of Cu element in Fig. 1c except the strong peaks of Au element. The reason is that Au segments have a length of about 2μm, but the electron beam reaching on the sample forms a large region. The diameter of electron beam exceeds 2μm that Cu segments are involved, so the characteristic X rays of Cu are induced together with Au as a result.

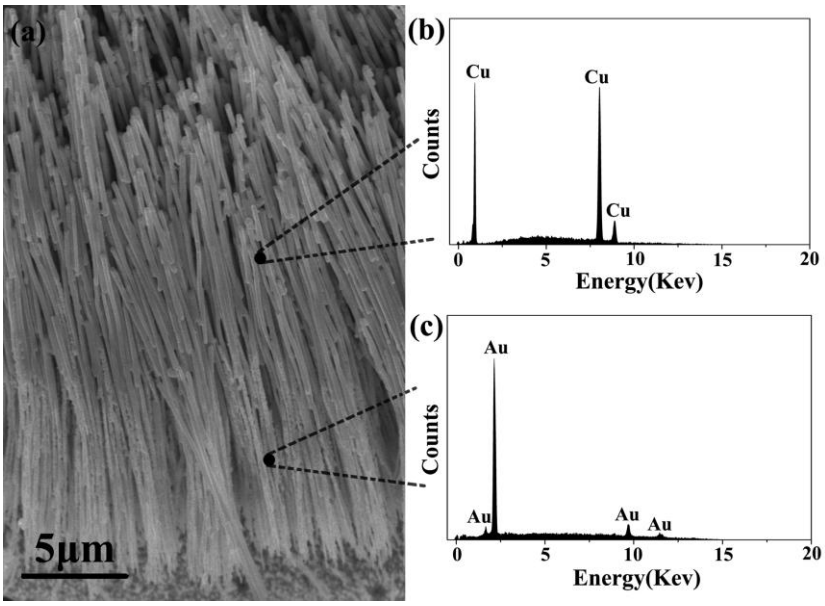

Figure 2. SEM image (a) and EDS patterns (b) (c) of the as-prepared Au-Cu heterojunction nanowires from d_N = 20 nm AAO

Au-Cu heterojunction nanowires fabricated from AAO template of d_N = 20 nm are shown in Fig. 2. The nanowires are uniform and well-ordered and hold a length of 20 μm. Au segments at the

bottom have a length of 10 μm, which is as long as that of the Cu segments. The diameter of the nanowires is about 140 nm, which is decided by the commercial template [29]. It is shown clearly that Au segments are composed of large particles and exhibit a rough surface, while Cu segments show a smooth surface. The great structure difference makes a distinct interface between Au segments and Cu segments. The elemental compositions of the Au-Cu nanowires are evidenced by the EDS spectra, which are corresponding to the positions shown in Fig. 2a.

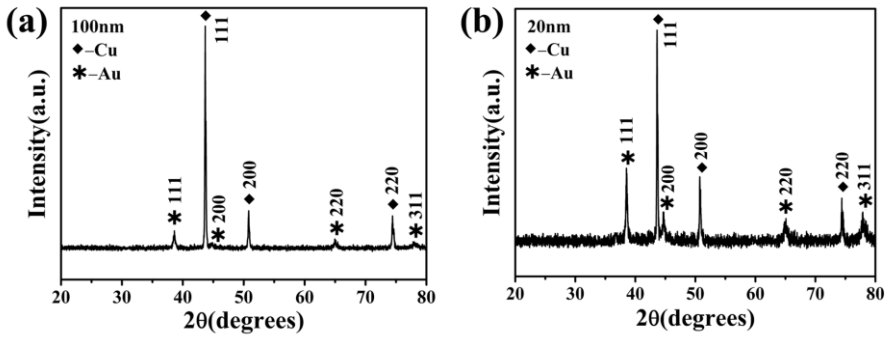

Figure 3. XRD patterns of the as-prepared Au-Cu heterojunction nanowires from (a) AAO of d_N = 100 nm and (b) AAO of d_N = 20 nm

XRD patterns of the Au-Cu heterojunction nanowires synthesized in AAO template of different diameters are shown in Fig. 3. The XRD patterns clearly show that the two samples reveal common polycrystalline structures. By comparing the data with standard powder diffraction pattern of Au and Cu, it is found that the intensity of peak (111) is the highest in the prepared samples, indicating that there was a preferred orientation during the growth of nanowires. The diffraction peaks in XRD patterns shown in Fig. 3 are well-indexed to the cubic Au [32] and cubic Cu [33] structures (JCPDS cards Au: No.04-0784; Cu: No.04-0836). This structural characterization further confirms that the heterojunction structure of Au-Cu nanowires was formed in the process of electrodeposition.

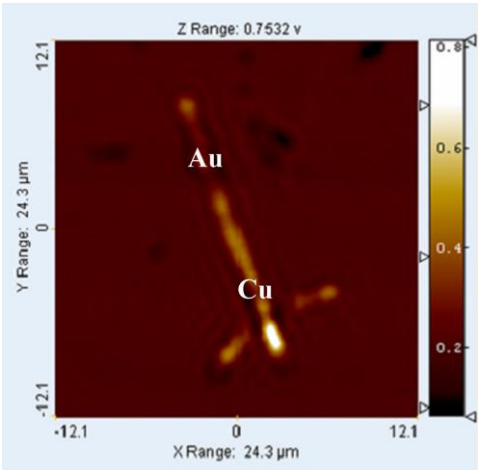

Figure 4. Reflected laser confocal image of a single Au-Cu heterojunction nanowire deposited within d_N = 20 nm AAO

Reflected laser confocal image of an individual Au-Cu heterojunction nanowire deposited in d_N = 20 nm AAO showing in Fig. 4 further confirms the formation of Au-Cu heterojunction structure. From the very different brightness contrast, it is concluded that there are different metals (labeled as Au and Cu) along the nanowire. The differences between brightness and contrast are due to different reflectivity of Au and Cu. Compared with Cu segment which has a smooth surface, Au segment is consisted of obvious large particles (Fig. 2a). These large particles absorb incident light and make the Au segment darker than Cu segment.

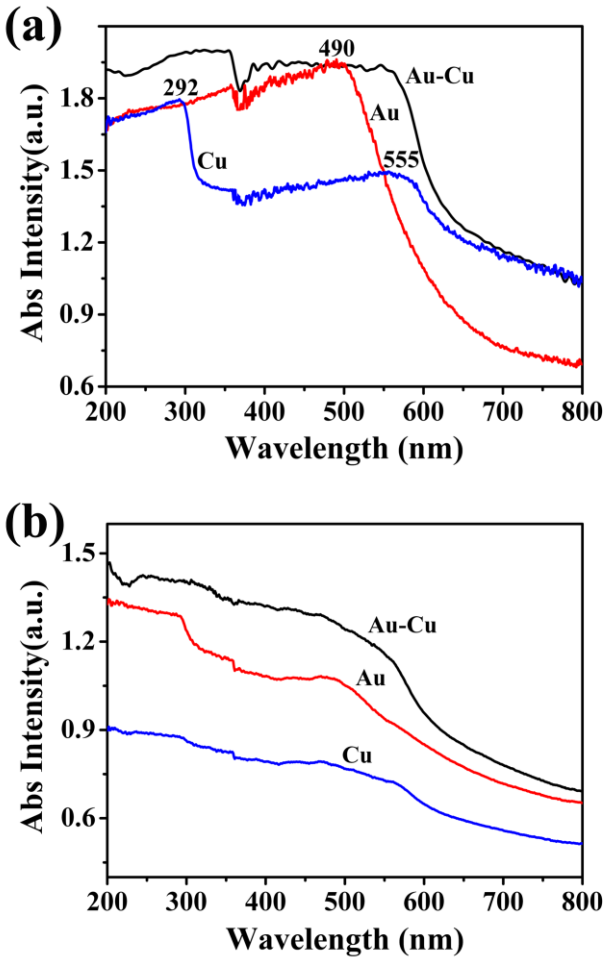

Figure 5. UV-visible absorption spectra of Au, Cu, and Au-Cu heterojunction nanowires deposited in AAO template of different diameters (a) d_N = 100 nm and (b) d_N = 20 nm

UV-visible absorption spectra of the Au-Cu heterojunction nanowires were compared with single Au nanowires and Cu nanowires. The absorption spectrum of nanowires made from the AAO template of d_N = 100nm is shown in Fig. 4a. A wide absorption band around 490 nm is observed for Au nanowires. For Cu nanowires, two absorption bands appear and one is around 555 nm and the other at 292 nm which locates in the UV region. In comparison to the single Au and Cu nanowires, no obvious absorption peaks but a wide and enhanced absorption band between 200 and 550 nm appear in the absorption spectrum of Au-Cu heterojunction nanowires. The absorption spectrum of nanowires

made from d_N = 20 nm AAO (Fig. 4b) reveals similar results compared with the d_N = 100 nm nanowires. The Au-Cu heterojunction nanowires exhibit an absorption band between 200 nm and 600 nm which is enhanced and band edge red-shifted compared with the single Au and Cu nanowires.

Strong interfacial coupling between Au and Cu can be the reason for broadening, enhancement and red shift of surface plasmon absorption of the Au-Cu heterojunction nanowires. It is attributed to the electron transfer between Au and Cu segments [34]. To further account for the electron transfer between Au and Cu, relationship of the position of plasmon absorption on the electron density of metal is adopted [35], which is given as follows

$$\lambda = [4\pi^2 c^2 m_{eff}\varepsilon_0/Ne^2]^{1/2} \qquad (1)$$

where λ is the plasmon absorption wavelength and N is the electron density of metal materials. The work function of Cu is at about 4.65 eV and the work function of Au is around 5.1eV. The Fermi energy level of Cu is higher than that of Au due to its smaller work function, so that electron transfer occurs from Cu to Au during the formation of Au-Cu heterojunction nanowires, resulting in a uniform Fermi energy level in the heterojunction structure. Therefore, the deficient electrons on the surface of the Cu segments subsequently lead to the broadening and red shift of the surface plasmon absorption according to the above formula. The enhanced absorption of the Au-Cu heterojunction nanowires is due to the surface plasmon resonance between the Au and Cu segments for their close surface plasmon absorption.

4. CONCLUSIONS

Using the AAO template combined with electrochemical deposition, the Au-Cu heterojunction nanowires with different diameters were prepared. The orderly nanowires were controlled by proper deposition parameters and their aspect ratios were manipulated by adjusting the diameters of AAO and deposition duration. SEM, XRD, EDS and reflected laser confocal imaging were conducted to confirm the Au-Cu heterojunction structure. Optical properties were studied for the fabricated nanowires. The Au-Cu heterojunction nanowires exhibit wide and strong absorption bands in UV-visible absorption spectra due to the strong interfacial coupling between Au and Cu segments. Due to the unique structure, simple synthetic method and unique properties, the Au-Cu heterojunction nanowires are expected to provide new insights in device integration, catalytic and biological applications.

ACKNOWLEDGMENTS
This work was financially supported by National Basic Research Program of China (2009CB930503), NSFC (Contract No. 51021062), the Fund for the Natural Science of Shandong Province (ZR2010EM020, ZR2010EM049) and IIFSDU (2012JC007).

References

1. G. Schider, J.R. Krenn, W. Gotschy, B. Lamprecht, H. Ditlbacher, A. Leitner, F.R. Aussenegg, J *Appl Phys*, 90 (2001) 3825.

2. R.L. Zong, J. Zhou, Q, Li, B. Du, B. Li, M. Fu, X.W. Qi, L.T. Li, S. Buddhudu, *J Phys Chem B,* 108 (2004) 16713.
3. W.R. Hendren, A. Murphy, P. Evans, D. O'Connor, G.A. Wurtz, A.V. Zayats, R. Atkinson, R.J. Pollard, *J Phys-Condens Mat,* 20 (2008) 362203.
4. C.M. Hangarter, N.V. Myung, *Chem Mater*, 17 (2005) 1320.
5. L. Piraux, J.M. George, J.F. Despres, C. Leroy, E. Ferain, R. Legras, K. Ounadjela, A. Fert, *Appl Phys Lett,* 65 (1994) 2484.
6. J.J. Mock, S.J. Oldenburg, D.R. Smith, D.A. Schultz, S. Schult, *Nano Lett,* 2 (2002) 465.
7. S. Kim, S.K. Kim, S. Park, *J Am Chem Soc,* 131 (2009) 8380.
8. M. Tanase, D.M. Silevitch, A. Hultgren, L.A. Bauer, P.C. Searson, G.J. Meyer, D.H. Reich, *J Appl Phys,* 91 (2002) 8549.
9. J.G. Wang, M.L. Tian, T.E. Mallouk, M.H.W. Chan, *Nano Lett*, 4 (2004) 1313.
10. A. Blondel, J.P. Meier, B. Doudin, J.P. Ansermet, *Appl Phys Lett*, 65 (1994) 3019.
11. S. Dubois, C. Marchal, J.M. Beuken, L. Piraux, J.L. Duvail, A. Fert, J.M. George, J.L. Maurice, *Appl Phys Lett,* 70 (1997) 396.
12. H.M. Zhang, Y.G. Guo, L.J. Wan, C.L. Bai, *Chem Commun,* 24 (2003) 3022.
13. F. Liu, J.Y. Lee, W.J. Zhou, *Adv Funct Mater,* 15 (2005) 1459.
14. S.H. Yoo, S. Park, *Adv Mater,* 19 (2007) 1612.
15. S. Park, J.H. Lim, S.W. Chung, C.A. Mirkin, *Science,* 303 (2004) 348.
16. S.R. Nicewarner-Pena, R.G. Freeman, B.D. Reiss, L. He, D.J. Pena, I.D. Walton, R. Cromer, C.D. Keating, M.J. Natan, *Science,* 294 (2001) 137.
17. I.D. Walton, S.M. Norton, A. Balasingham, L. He, D.F. Oviso, D. Gupta, P.A. Raju, M.J. Natan, R.G. Freeman, *Anal Chem,* 74 (2002) 2240.
18. C. Della Pina, E. Falletta, M. Rossi, *J Catal,* 260 (2008) 384.
19. X. Liu, A. Wang, X. Wang, C.Y. Mou, T. Zhang, *Chem Commun*, 27 (2008) 3187.
20. J. Llorca, M. Dominguez, C. Ledesma, R.J. Chimentao, F. Medina, J. Sueiras, I. Angurell, M. Seco, O. Rossell, *J Catal*, 258 (2008) 187.
21. W. Chen, R. Yu, L. Li, A. Wang, Q. Peng, Y. Li, *Angew Chem Int Edit,* 49 (2010) 2917.
22. A. Henkel, A. Jakab, G. Brunklaus, C. Soennichsen, *J Phys Chem C,* 113 (2009) 2200.
23. Y. Liu, A.R.H. Walker, *Angew Chem Int Edit,* 49 (2010) 6781.
24. A.K. Sra, T.D. Ewers, R.E. Schaak, *Chem Mater,* 17 (2005) 758.
25. L. Shi, A. Wang, Y. Huang, X. Chen, J. Jose Delgado, T. Zhang, *Eur J Inorg Chem,* 16 (2012) 2700.
26. M.J. Zheng, L.D. Zhang, G.H. Li, W.Z. Shen, *Chem Phys Lett*, 363 (2002) 123.
27. S.J. Hurst, E.K. Payne, L.D. Qin, C.A. Mirkin, *Angew Chem Int Edit*, 45 (2006) 2672.
28. M.R. Kim, D.K. Lee, D.J. Jang, *J Nanomater,* (2010) 203756.
29. C. Schonenberger, B.M.I. van der Zande, L.G.J. Fokkink, M. Henny, C. Schmid, M. Kruger, A. Bachtold, R. Huber, H. Birk, U. Staufer, *J Phys Chem B,* 101 (1997) 5497.
30. P. Forrer, F. Schlottig, H. Siegenthaler, M. Textor, *J Appl Electrochem,* 30 (2000) 533.
31. T.S. Ramulu, R. Venu, B. Sinha, S.S. Yoon, C.G. Kim, *Int J Electrochem Sci*, 7 (2012) 7762.
32. S. Habouti, M, Matefi-Tempfli, C.H. Solterbeck, M. Es-Souni, S. Matefi-Tempfli, M. Es-Souni, *Nano Today,* 6 (2011) 12.
33. T. Gao, G.W. Meng, J. Zhang, Y.W. Wang, C.H. Liang, J.C. Fan, L.D. Zhang, *Appl Phys A-Mater,*73 (2001) 251.
34. T. Singh, D.K. Pandya, R. Singh, *Thin Solid Film,* 520 (2012) 4646.
35. Y. Liu, M. Zhong, G. Shan, Y. Li, B. Huang, G. Yang, *J Phys Chem B,* 112 (2008) 6484.